Arabian Journal of Geosciences (2021) 14: 64
https://doi.org/10.1007/s12517-020-06446-9

ORIGINAL PAPER

Natural radioactivity measurements and evaluation of radiological hazards in sediment of Aliağa Bay, İzmir (Turkey)

Selin Özden[1] · Serpil Aközcan[1]

Received: 20 August 2020 / Accepted: 30 December 2020 / Published online: 13 January 2021

Abstract

The activity concentration of natural ^{226}Ra, ^{232}Th, and ^{40}K radionuclides was examined in some selected locations in Aliaga Bay of Izmir district, Turkey. Sediment samples from 30 locations were collected and analyzed for radionuclides activity concentration by gamma-ray spectrometry using a high-purity germanium HPGe gamma-ray detector. The activity concentrations of the sediment samples range from 23.5 ± 1.7 to 59.5 ± 1.6 Bq kg^{-1} for ^{226}Ra, 37.5 ± 0.9 to 64.4 ± 0.6 Bq kg^{-1} for ^{232}Th, and 354.7 ± 5.6 to 978.4 ± 5.8 Bq kg^{-1} for ^{40}K. Based on the obtained results, the radiological parameters were evaluated. The mean values for absorbed dose rate, annual effective dose equivalent, radium equivalent activity, external hazard index, and excess lifetime cancer risk were determined and found as 81.64 nGy h^{-1}, 100.13 μSv y^{-1}, 173.31 Bq kg^{-1}, 0.47, and 0.40, respectively. Calculated radiological parameters of sediment samples were compared with the World Standard Value. The results obtained in this study were found to be above the globally standard limit for most locations. Statistical data such as skewness and kurtosis were calculated, and frequency distribution, Pearson's correlation analysis, box plot, factor analysis, and cluster analysis were applied in order to assess the distribution of radiological parameters and relationship between them.

Keywords Natural radioactivity · Radionuclides · Radiological hazards · Sediment · Statistical approach

Introduction

In the nature, radionuclides can be found as primordial, cosmogenic, and human-produced. Primordial radionuclides are present from the origin of the earth, cosmogenic radionuclides form as a result of cosmic ray interaction, and human-produced radionuclides come up with human activities such as nuclear weapon tests in the atmosphere, various applications of medicine, industries, and consumer products (Shouop et al. 2017; Khan et al. 2010). Natural environmental radioactivity develops principally from primordial radionuclides such as ^{232}Th and ^{238}U and their product of decay as well as ^{40}K.

People are exposed to both external and internal radiation due to naturally occurring radionuclides that are present since the creation of the earth (Altunsoy et al. 2020; Al-Obaidi et al. 2020). Naturally occurring radionuclides are present in soil, rock, water, plant, sand, and air (SureshGandhi et al. 2014; Özseven et al. 2020; Akkurt et al. 2015; Albidhani et al. 2019). They are not uniformly distributed depending on the geographical conditions and geological formations in each region in the world. The activity of naturally existing radionuclides in sediment and also soil change depend on the type of rock from which they originate (Huang et al. 2015; Tzortzis et al. 2004; Agbalagba et al. 2014). Radionuclides in marine sediment dissolve in water over time and transfer to plants, animals, and human. The knowledge of concentration and distribution of natural radionuclides in sediment is crucial since the level of activity concentration influences human exposure to radiations. Many studies were performed on natural radioactivity in the literature (Kulalı et al. 2019; Günay et al. 2019; Günay et al. 2018a; Günay et al. 2018b; Külahçı et al. 2020; Günay and Eke 2019; Günay 2018; Mavi and Akkurt 2010; Nevinsky et al. 2018; Özseven et al. 2020).

In this study, sediment samples were collected from Aliaga Bay and analyzed to identify natural ^{226}Ra, ^{232}Th, and ^{40}K gamma-emitting radionuclides. Aliaga Bay is located in the central Eastern Aegean Sea and has been contaminated by extensive domestic and industrial pollution load (Pazi et al. 2017). Aliaga region is located at about 50 km far from the north of Izmir in the western part of Turkey. The oldest rock

✉ Selin Özden
selinnozden@gmail.com

[1] Faculty of Science and Literature, Department of Physics, Campus of Kayali, Kirklareli University, Kirklareli, Turkey

unit of Aliaga is the Izmir flysch deposits of Cretaceous age. The main rocks that are exposed in the outcrop are volcano–sedimentary rocks including limestone, silicified limestone, marl, andesite, basalt, tuff, and tuffite of the Upper Miocene age and volcanic rocks of the Pliocene age (Sponza and Karaoğlu 2002). The town has a population of about 60,000 and the economy is mainly based on an oil refinery and also cultural tourism. Various industrial facilities are located in Aliaga Bay especially Tupras (the second largest oil refinery of Turkey), Petkim (a petro chemistry plant), iron–steel facilities, shipbreaking facilities, phosphate fertilizer plant, paper factory, and two thermal power plants based on natural gas. Industrial activities associated with these facilities cause environmental pollution in this region. In addition, the industrial plants in Aliaga cause marine pollution and change the natural balance of the sea (Arslan et al. 2015; Neşer et al. 2012). In several areas of Aliaga, rivers (especially Bakırçay River) and bays have been polluted by industrial and agricultural human activities, or waste disposal. Along its path, the Bakırçay River basin includes several agricultural lands where the farmers use often the fertilizers. Natural radionuclides are released to the environment in several industrial activities such as minerals mining, beneficiation and chemical processing of ores, phosphate fertilizer production and use, and fossil fuel combustion, causing enhanced natural radiation exposures etc. (Çam et al. 2013).

The objective of this study is to evaluate the radiological hazard in Aliaga Bay of Izmir district. Absorbed dose rate, annual effective dose equivalent, radium equivalent activity, external hazard index, and excess lifetime cancer risk were determined and compared to the limits given by the United Nations Scientific Committee on the Effects of Atomic Radiation (UNSCEAR 2000). The parameters obtained in this investigation may contribute to the natural radioactivity level database, and give information about the activity distribution of natural radionuclides and the radiation doses to human beings in contact with this area.

Materials and methods

Sample collection and preparation

The sediment samples were collected manually from the surface layer sediment of 10-cm depth. The surface sediment samples were collected from 30 different locations (Fig. 1). The collected samples were then placed in labeled polythene bags and transferred to the laboratory for preparation and analysis. After that, the sediment samples were sieved through a 2-mm mesh. Then the samples were dried at 105 °C for 24 h and placed in polyethylene containers. Samples were stored in polyethylene containers for more than 4 weeks to reach secular equilibrium between ^{226}Ra and its daughters/decay products (Ergül et al. 2013; Aközcan 2014).

Activity measurements

The gamma spectra of the surface sediment samples were collected in the laboratory at the Central Research Laboratory of Kırklareli University by HPGe detector (Ortec, USA) with a 70% relative efficiency in multilayer shielding. The detector used was connected to a computer program MAESTRO window that matched the gamma energies to a library of possible isotopes and analyses were performed by GammaVision-32 software program. The gamma-ray peak of the 911.2 keV from ^{228}Ac and the 583.1 keV from ^{208}Tl was used to determine the activity concentration of ^{232}Th in the sediment samples. The activity concentration of ^{226}Ra was determined using gamma-ray lines at 351.9 keV for ^{214}Pb and 609.3 keV for ^{214}Bi, respectively. The activity concentration of ^{40}K was evaluated using gamma-ray line at 1460.8 keV. The energy and efficiency calibrations of the detector were performed using multinuclide reference source (Isotope Products Laboratories, volume: 1.300 mL, density: 1.0 g cm^{-3}) in 250-mL cylindrical geometry.

The mixed radionuclide, in the form of epoxy used for the calibration, contained 11 radionuclides in the energy range of 60–1836 keV as ^{210}Pb, ^{241}Am, ^{109}Cd, ^{57}Co, ^{139}Ce, ^{203}Hg, ^{113}Sn, ^{85}Sr, ^{137}Cs, ^{88}Y, and ^{60}Co. The efficiency calibration of the HPGe detector was also carried out using the six different radionuclides (namely ^{241}Am, ^{109}Cd, ^{57}Co, ^{137}Cs, and ^{60}Co) obtained in the spectrum. Out of the six radionuclides, four radionuclides reformed the fit of the data and the two discarded. The following radionuclides were used for the efficiency calibration: ^{57}Co (122 keV), ^{137}Cs (662 keV), ^{60}Co (1173 keV), and ^{57}Co (1333 keV). The resolution of the detector was determined by measuring a standard ^{137}Cs source on the detector and a spectrum of the full energy peak located at 662 keV. Each sample and the background were counted for 160000 s (44 h). The activity concentration of ^{226}Ra, ^{232}Th, and ^{40}K in the measured samples is calculated by the following relation (Aközcan et al. 2018);

$$A\left(\mathrm{Bg\,kg^{-1}}\right) = \frac{\mathrm{CPS}}{\mathcal{E} \times M \times I_{\gamma}} \quad (1)$$

where A represents the specific activity, CPS is the net gamma counting rate (counts per seconds), ε is the detector efficiency of a specific gamma ray, $I\gamma$ is the gamma-ray emission probability, and M is the mass of the sample (kg).

The minimum detectable activity (MDA) of the γ-ray measurement system was calculated using the following equation (Currie 1968):

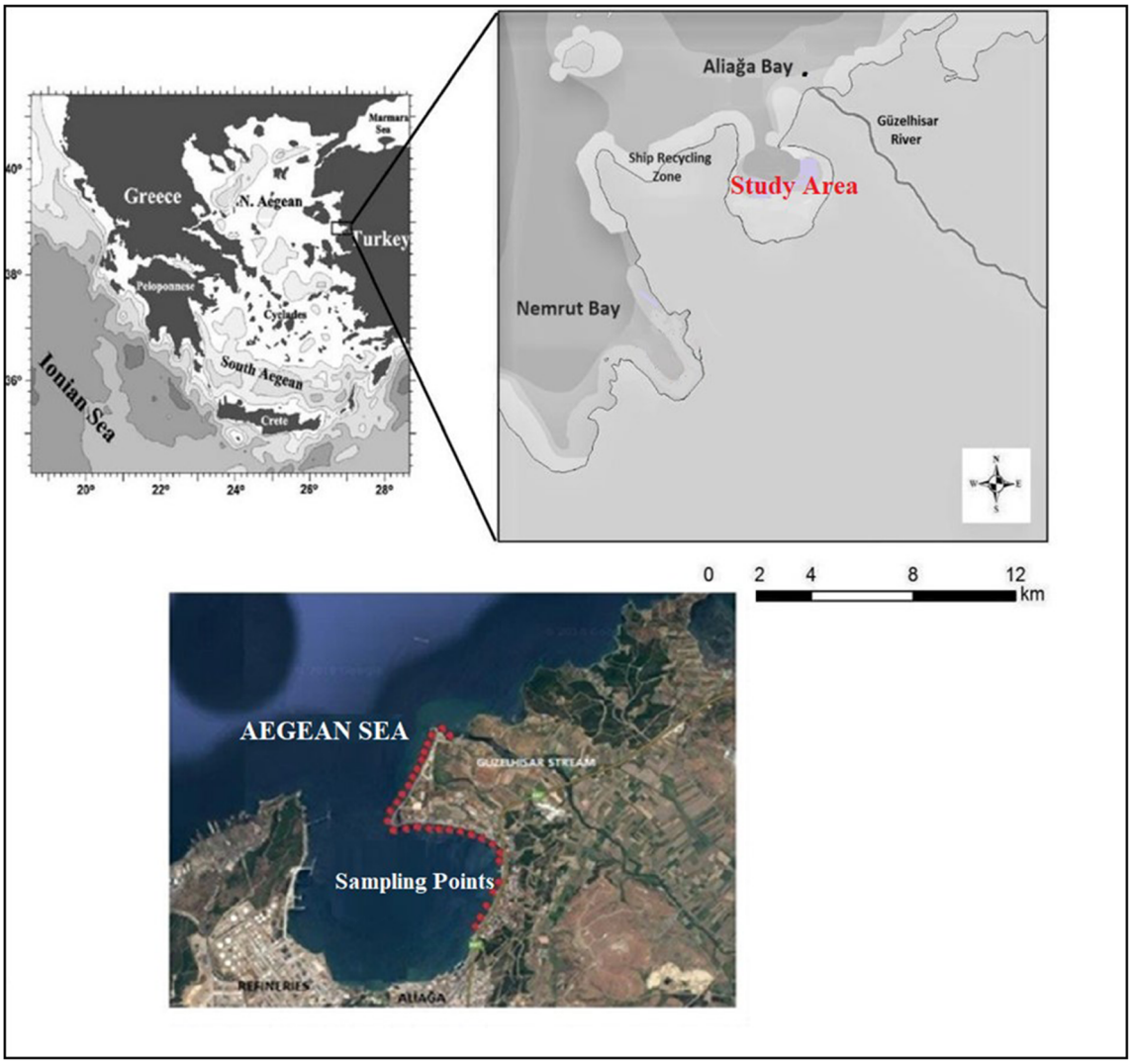

Fig. 1 Sample collection sites around Aliaga Bay (Eastern Aegean Sea) (Aydın et al. 2015)

$$\mathrm{MDA} = \frac{2.71 + 4.65B^{1/2}}{\mathcal{E} \times t} \tag{2}$$

where B is the background counts, $\mathcal{E}$ is the counting efficiency, and t is the counting time in seconds (Aközcan et al. 2014).

The minimum detectable activities (MDAs) were 2.75 Bq kg^{-1} for ^{40}K, 0.7 Bq kg^{-1} for ^{232}Th, and 0.9 Bq kg^{-1} for ^{226}Ra.

Evaluation of radiological parameters

Absorbed dose rate (*D*)

The absorbed dose rate, D (nGy h^{-1}), due to terrestrial gamma radiations in air at 1 m above the ground level, was calculated using the Eq. (3) (Aközcan et al. 2018; UNSCEAR 2000; Alajeeli et al. 2019).

$$D\left(\mathrm{nGyh}^{-1}\right) = 0.462C_{\mathrm{Ra}} + 0.604C_{\mathrm{Th}} + 0.0417C_{\mathrm{K}} \tag{3}$$

where C_{Ra}, C_{Th}, and C_{K} are the massic activities of ^{226}Ra, ^{232}Th, and ^{40}K in the sediment samples, respectively. 0.462, 0.604, and 0.0417 are the conversion factors for ^{226}Ra, ^{232}Th, and ^{40}K to evaluate the absorbed dose rate in air per unit specific activity in becquerels per kilogram (dry weight).

Annual effective dose equivalent

The annual effective dose equivalent received by human due to natural radioactivity in the sediment samples was calculated using the Eq. (4) (UNSCEAR 2000).

$$\mathrm{AEDE}\left(\mu\mathrm{Sv\ y}^{-1}\right) = D\left(\mathrm{nGy\ h}^{-1}\right) \times 8760\left(\mathrm{hy}^{-1}\right) \times 0.2 \times 0.7\left(\mathrm{SvGy}^{-1}\right) \times 10^{-3} \tag{4}$$

where D is the absorbed dose rate, 0.7 Sv Gy^{-1} is the dose convention factor, 0.2 (5/24) is the outdoor occupancy factor, and 8760 is the hour per a year.

Radium equivalent activity

The distribution of radionuclides such as ^{226}Ra, ^{232}Th, and ^{40}K is not homogeneous in some area. Therefore, to compare the concentrations of these radionuclides and to evaluate the gamma radiation hazard to humans associated with the sediment samples, the radium equivalent activity (Ra_{eq}) in becquerels per kilogram was calculated according to the following relation given by Beretka and Mathew (Beretka and Mathew 1985):

$$Ra_{eq}\left(Bq\ kg^{-1}\right) = C_{Ra} + 1.43C_{Th} + 0.077C_K \quad (5)$$

where C_{Ra}, C_{Th}, and C_K are the massic activities of ^{226}Ra, ^{232}Th, and ^{40}K in the sediment samples, respectively. In this relation, it is assumed that 370 Bq kg^{-1} of ^{226}Ra, 259 Bq $kg^{-1}$of ^{232}Th, and 4810 Bq kg^{-1} of ^{40}K produce the same gamma dose rate.

External hazard index

The external hazard index gives an estimation the level of radiological risk of the samples and it must be less than unity to be free from the radiological hazards. The external hazard index was calculated for the sediment samples using the following formula which is proposed by Krieger (Krieger 1981; Al-Hamarneh and Awadallah 2009):

$$H_{ex} = \frac{C_{Ra}}{370} + \frac{C_{Th}}{259} + \frac{C_K}{4810} \quad (6)$$

where C_{Ra}, C_{Th}, and C_K are the massic activities of ^{226}Ra, ^{232}Th, and ^{40}K in the sediment samples, respectively. Krieger model assumes that the maximum value of the external hazard index is unity if the upper limit of Ra_{eq} equals to 370 Bq kg^{-1}.

The excess life time cancer risk

The excess life time cancer risk (ELCR) gives the probability of the cancer risk to any population over a lifetime caused by exposure to ionizing radiation. It was calculated for sediment samples by the following equation (Taskin et al. 2009; Kolo et al. 2017):

$$ELCR = AEDE\left(\mu Sv\ y^{-1}\right) \times DL\ (y) \times RF\left(Sv^{-1}\right) \quad (7)$$

where DL is the average life time duration (70 years) and RF is the risk factor which gives the fatal cancer risk per sievert. For stochastic effects, International Commission on Radiological Protection (ICRP) suggests the value of 0.057 for the public exposure (ICRP 2007).

Results and discussion

Activity concentrations

The activity concentrations of ^{226}Ra, ^{232}Th, and ^{40}K in the sediment samples collected from Aliaga Bay are given in Table 1. Figure 2, Fig. 3, and Fig. 4 show the activity

Table 1 The activity concentrations of ^{226}Ra, ^{232}Th, and ^{40}K in the sediment samples from Aliaga Bay

Sample Location	Activity concentration (Bq kg^{-1} in dry weight)		
	^{226}Ra	^{232}Th	^{40}K
1	23.54	38.25	416.53
2	25.23	37.54	478.96
3	30.28	45.68	354.71
4	26.53	47.28	487.52
5	39.57	50.46	469.31
6	49.41	52.78	563.34
7	50.08	49.13	756.84
8	52.31	48.97	600.31
9	47.62	49.76	784.52
10	41.02	55.76	614.25
11	50.97	49.78	698.74
12	46.89	42.41	650.31
13	55.87	47.82	687.41
14	39.14	48.69	741.25
15	42.52	50.16	705.34
16	49.85	47.89	800.41
17	40.94	41.66	879.36
18	42.58	44.25	747.96
19	58.27	43.89	879.63
20	55.86	49.74	896.34
21	47.28	47.16	713.68
22	39.65	50.69	746.35
23	42.56	55.61	806.78
24	45.21	48.63	888.63
25	52.47	60.14	945.63
26	56.45	54.78	741.79
27	52.87	59.87	978.35
28	55.13	62.34	974.12
29	59.46	61.47	845.52
30	58.74	64.37	784.13
Range	23.54–59.46	37.54–64.37	354.71–978.35
Average	45.94	50.23	721.27
World average	35	30	400

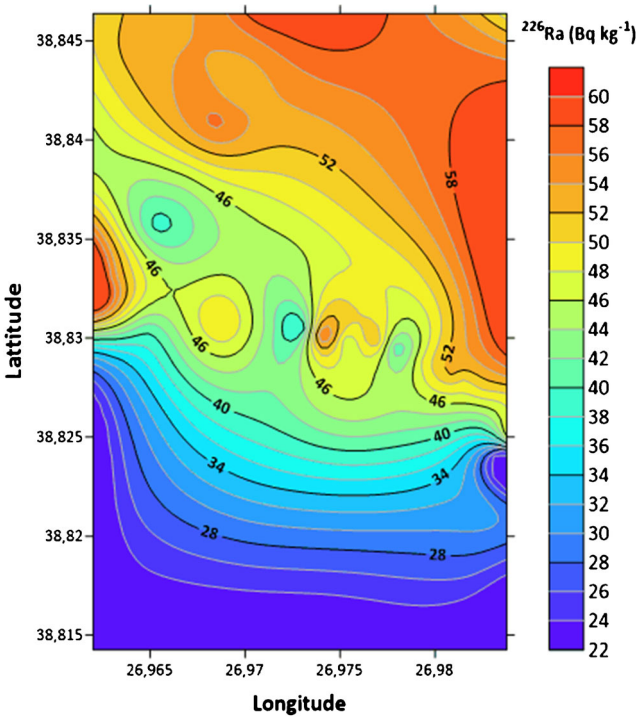

Fig. 2 ^{226}Ra activity concentration distribution in Bq kg^{-1} of sediment samples

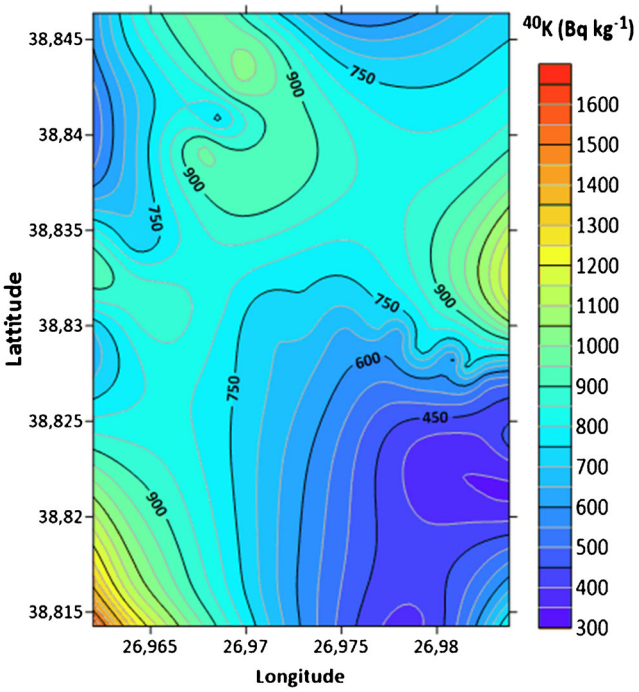

Fig. 4 ^{40}K activity concentration distribution in Bq kg^{-1} of sediment samples

concentration distribution maps of ^{226}Ra, ^{232}Th, and ^{40}K in the sediment samples respectively. The activity concentration results are given in becquerels per kilogram of dry weight. As clearly seen, the lowest ^{226}Ra activity concentration was found at location 1 (38° 48′ 51.4″ N, 26° 58′ 46.1″ E) whereas the highest was investigated at location 29 (38° 50′ 46.9″ N 26° 58′ 14.7″ E). The lowest ^{232}Th activity concentration was observed at location 2 (38° 49′ 03.6″ N, 26° 58′ 54.3″ E) and the highest one was found 30 (38° 50′ 44.2″ N 26° 58′ 19.5″ E). In addition, the highest ^{40}K activity was observed at location 27 (38° 50′ 33.5″ N 26° 58′ 09.9″ E) and the lowest value was at location 4 (38° 49′ 28.1″ N 26° 59′ 01.6″ E).

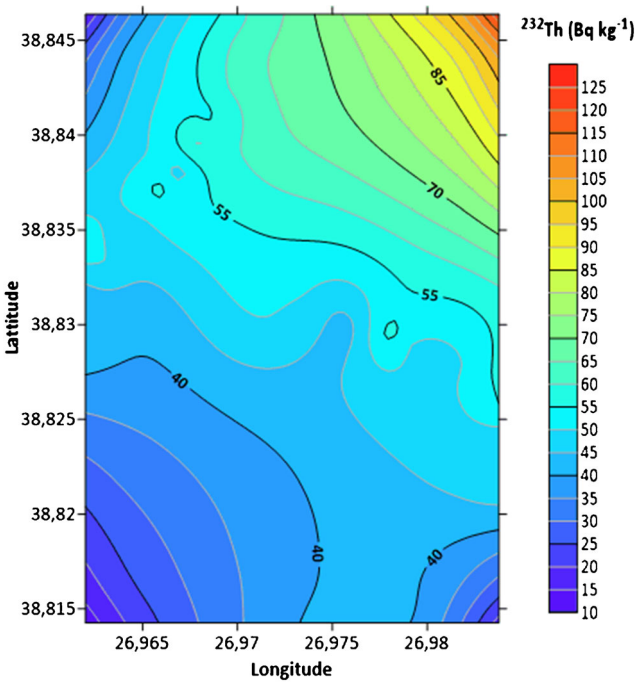

Fig. 3 ^{232}Th activity concentration distribution in Bq kg^{-1} of sediment samples

The results show that the mean activity of ^{226}Ra, ^{232}Th, and ^{40}K in sediments of Aliaga Bay is higher than the world average as given in Table 1 (UNSCEAR 2000). The activity concentrations of radionuclides are compared with other studies for sediment samples in Table 2. As shown in the table, the range of activity concentration of ^{226}Ra is much higher than the values reported for Spain (9–14 Bq kg^{-1}) and Kuwait Bay (19–21 Bq kg^{-1}) (Ligero et al. 2001; Zamel et al. 2005). The ^{232}Th activity concentrations reported in Italy (31–37 Bq kg^{-1}) and Spain (11–16 Bq kg^{-1}) are lower than our values (Ligero et al. 2001; Doretti et al. 1992). The maximum value of ^{40}K activity in the present study is much higher than the values reported for Albania (675 Bq kg^{-1}), Egypt (487 Bq kg^{-1}), Italy (475 Bq kg^{-1}), Spain (460 Bq kg^{-1}), Pakistan (825 Bq kg^{-1}), and Kuwait Bay (683 Bq kg^{-1}), but lower than Greece (1593 Bq kg^{-1}), Rize/Turkey (1605 Bq kg^{-1}), Bafa Lake/Turkey (1092 Bq kg^{-1}), and Aqaba Gulf (1133 Bq kg^{-1}).

Sediment samples have different physical, chemical, and geological structure and location characteristics; therefore, the obtained results vary. Natural radioactivity levels of sediments vary from place to place depending upon the concentration of

Table 2 Comparison of natural radioactivity of Aliaga Bay sediments with other areas of the world

Area	^{226}Ra (Bq kg^{-1})	^{232}Th (Bq kg^{-1})	^{40}K (Bq kg^{-1})	References
Albania	13–23	13–40	266–675	Tsabaris et al. 2007
Egypt	4–48	8–50	16–487	Ibraheim et al. 1995
Greece	19–81	19–88	152–1593	Florou and Kritidis 1992
Italy	–	31–37	410–475	Doretti et al. 1992
Spain	9–14	11–16	220–460	Ligero et al. 2001
Rize (Turkey)	15–116	17–87	51–1605	Kurnaz et al. 2007
Kucuk Menderes River Basin (Turkey)	13–73	11–58	235–1059	Aközcan 2014
Bafa Lake (Turkey)	30–73	32–66	332–1092	Yümün and Kam 2017
Pakistan	21.37–110.51	11.65–172.06	173.96–825.43	Qureshi et al. 2014
Aqaba Gulf	5.18–29.25	5.28–58.87	324.55–1133.04	Al–Trabulsy et al. 2011
Kuwait Bay	19–21	–	341–683	Zamel et al. 2005
Aliaga (Turkey)	24–60	38–64	355–978	Present study
UNSCEAR	35	30	400	UNSCEAR 2000

^{226}Ra, ^{232}Th, and ^{40}K present in rock and soil (Lu et al. 2016). Moreover, some agricultural activities (e.g., phosphate fertilizer usage) and industrial activities (e.g., phosphate fertilizer manufacture, coal-fired power plants, and cement production) in the river and sea valley may affect the natural radioactivity level of the sediment. The use of agricultural raw materials and industrial plants may affect the results. The agricultural phosphate fertilizer industries use raw materials that consist of phosphate rocks, phosphoric acid, ammonium phosphate, ammonium sulfate, dolomite, limestone, potassium ores (potassium sulfate, potassium chloride), and nitrogen-based compounds (ammonium nitrate, nitric acid), as plant growth depends mainly on nitrogen, phosphorus, and potassium. Phosphate ores, especially sedimentary ores, can be significantly enriched with naturally occurring radionuclides, uranium (^{238}U), and the daughter radionuclides coming from the radioactive decay of ^{238}U. Phosphate fertilizers are one of the most used materials in the agricultural field all over the world. The use of potassium-rich fertilizers has enriched the potassium content of the soil. The transport of potassium-rich soils to the sea by erosion appears to increase ^{40}K in the sediment. The use of fertilizers in large extent has affected radionuclide concentration, especially potassium-containing fertilizers are one of the causes of presence of high activity of ^{40}K in soil. Evidence of high ^{40}K activity in some sediment samples may indicate excessive use of phosphate fertilizer in agricultural lands and its transport to sediments (Yümün and Kam 2017; Boukhenfouf and Boucenna 2011; Ghosh et al. 2008). And also, the distributions of the natural radionuclides in the soils and sediments are closely related to the underlying geology. The Aliaga limestones form the sedimentary equivalents of the volcanic association (Çam et al. 2013). Although the distribution of ^{232}Th massic activity in the studied area shows similarity to that of ^{226}Ra, the relatively high values of ^{232}Th correspond well with volcanic rocks.

Radiological parameters

Radiological parameters were used to assess the effects of radiation on the health of people exposed to the radiation and the environment. In Table 3, the results obtained for the absorbed dose rate in air due to gamma radiation (D), the outdoor annual effective dose rate (AEDE), the radium equivalent activity (Ra_{eq}), and the external hazard index (H_{ex}), as well as the excess life time cancer risk (ELCR) assessment for sediment are presented. In addition, comparison of calculated absorbed dose rate, annual effective dose equivalent, radium equivalent activity, and excess lifetime cancer risk of sediment samples collected from Aliaga Bay with the World Standard Values is given in Fig. 3. As seen in Table 3, the absorbed dose rate ranged from 51.35 to 103.74 nGy h^{-1}. The average absorbed dose rate was calculated as 81.64 nGy h^{-1} which is higher than the world average absorbed dose rate of 57 nGy h^{-1} (UNSCEAR 2000).

In the present work, the calculated values of annual effective dose due to natural radioactivity ranged from 62.98 to 127.23 μSv y^{-1} with a mean value of 100.13 μSv y^{-1}, which is higher than the world average of 70 μSv y^{-1} (UNSCEAR 2000). It is observed that the values of D and AEDE for the studied sediment samples have higher values than world average value, except sample locations (1, 2, and 3) which have lower than world average (Fig. 5). The high absorbed dose rate in air and annual effective dose equivalent due to gamma radiation at collection sites were due to high level of ^{226}Ra, ^{232}Th, and ^{40}K in the surface sediments.

Table 3 Radiological parameters of sediment samples

Sample location	Absorbed dose rate, D (nGy h^{-1})	Annual effective dose equivalent, AEDE (μSv y^{-1})	Radium equivalent activity, Ra_{eq} (Bq kg^{-1})	External hazard index, H_{ex}	Excess life time cancer risk, ELCR ($\times 10^{-3}$)
1	51.35	62.97	110.31	0.30	0.25
2	54.30	66.60	115.79	0.31	0.27
3	56.37	69.13	122.92	0.33	0.28
4	61.14	74.99	131.68	0.36	0.30
5	68.33	83.80	147.86	0.40	0.33
6	78.20	95.90	168.26	0.45	0.38
7	84.37	103.47	178.61	0.48	0.41
8	78.78	96.61	168.56	0.46	0.39
9	84.77	103.96	179.18	0.48	0.41
10	78.24	95.96	168.05	0.45	0.38
11	82.75	101.49	175.96	0.48	0.40
12	74.40	91.24	157.61	0.43	0.36
13	83.36	102.23	177.18	0.48	0.41
14	78.40	96.15	165.84	0.45	0.38
15	79.35	97.32	168.56	0.46	0.39
16	85.33	104.65	179.96	0.49	0.42
17	80.75	99.03	168.22	0.45	0.40
18	77.59	95.16	163.45	0.44	0.38
19	90.11	110.51	188.76	0.51	0.44
20	93.23	114.33	196.01	0.53	0.46
21	80.09	98.22	169.67	0.46	0.39
22	80.06	98.18	169.61	0.46	0.39
23	86.89	106.57	184.20	0.50	0.43
24	87.32	107.08	183.18	0.49	0.43
25	99.99	122.64	211.28	0.57	0.49
26	90.10	110.50	191.90	0.52	0.44
27	101.38	124.34	213.82	0.58	0.50
28	103.74	127.23	219.28	0.59	0.51
29	99.86	122.46	212.47	0.57	0.49
30	98.72	121.06	211.17	0.57	0.48
Range	51.35–103.74	62.97–127.23	110.31–219.28	0.30–0.59	0.25–0.51
Average	81.64	100.13	173.31	0.47	0.40
World Average	57	70	370	–	0.29

The values of Ra_{eq} for the sediment samples varied from 110.31 to 219.28 Bq kg^{-1} and mean value of Ra_{eq} was found to be 173.31 Bq kg^{-1}. The mean value of the radium equivalent activity due to the activities of ^{226}Ra, ^{232}Th, and ^{40}K for the sediment samples is lower than the permissible value of 370 Bq kg^{-1} (UNSCEAR 2000). As seen in Fig. 3, all the Ra_{eq} values of samples are below the internationally accepted value 370 Bq kg^{-1} (UNSCEAR 2000).

The external hazard index varied from 0.29 to 0.59 with a mean value of 0.47. The calculated external hazard indices were less than the unity for all sampling locations which corresponds to the sediment samples which are free from the radiological hazards (Table 3).

The mean ELCR was found to be 0.40×10^{-3} and varied from 0.25×10^{-3} to 0.51×10^{-3}. The mean ELCR value was found to be higher than the world average ELCR value of 0.29×10^{-3} according to UNSCEAR (UNSCEAR 2000). As given in Fig. 3, the ELCR values for the studied sediment samples have higher values than the world average value, except sample locations (1, 2, and 3) which have lower than the world average (Fig. 5).

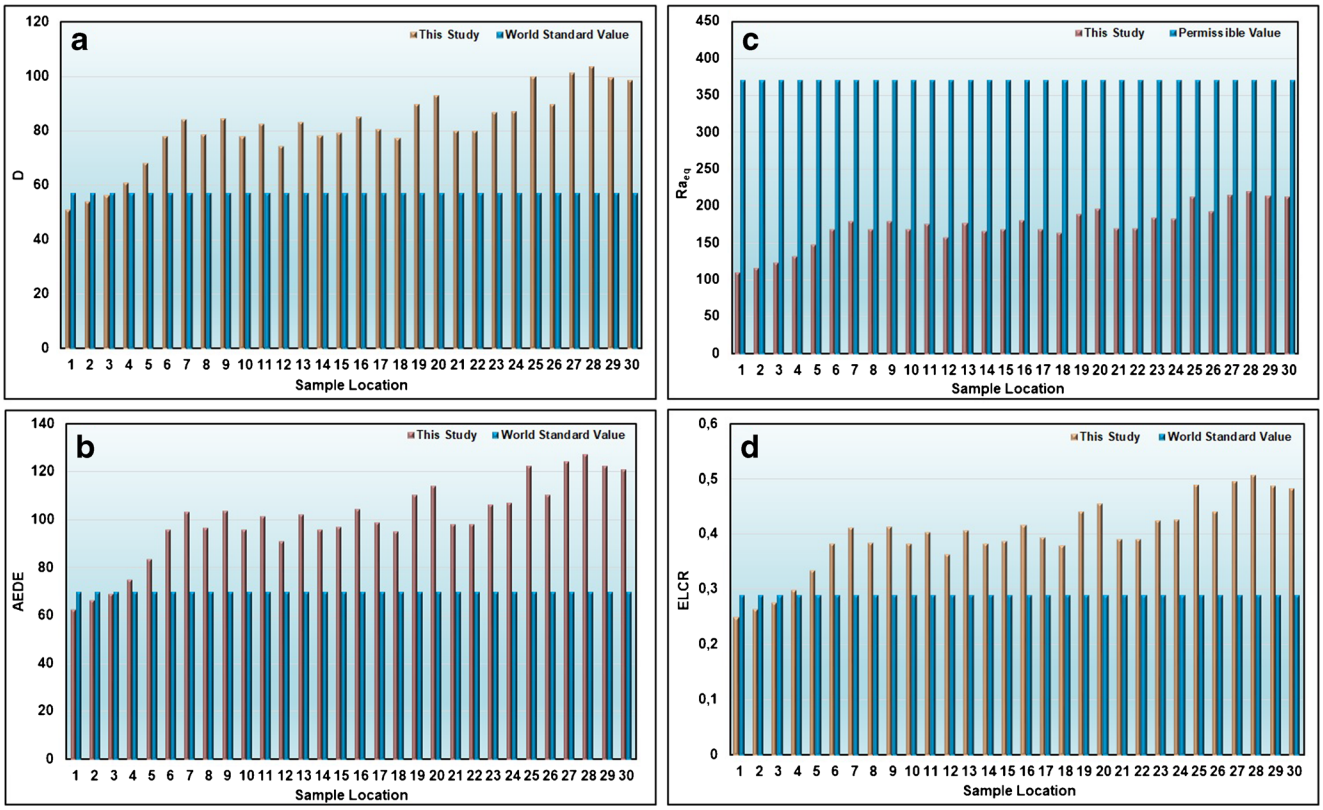

Fig. 5 Calculated **a** absorbed dose rate D (nGy h^{-1}), **b** annual effective dose equivalent AEDE (μSv y^{-1}), **c** radium equivalent activity Ra_{eq} (Bq kg^{-1}), and **d** excess lifetime cancer risk ELCR of sediment samples collected from Aliaga Bay and comparison with the World Standard and Permissible Value

Statistical approach

Statistical analysis of the activity concentrations of natural radionuclides was performed using statistical software (SPSS 25.0). Descriptive statistical data such as mean, median, kurtosis, skewness, and standard deviation for assessed parameters in sediment samples were calculated and are given in Table 4. Skewness of ^{226}Ra (− 0.79) and ^{40}K (− 0.51) was found to be negative while ^{232}Th was positive with 0.33. The positive and negative skewness values give the information about the asymmetric distribution. Negative values for the skewness of ^{226}Ra and ^{40}K indicate that the peak of the distribution is left of the mean value, and positive values for the skewness of ^{232}Th indicate that the peak of the distribution is right of the mean value. On the other hand, kurtosis values give information about the degree of peakedness of the probability distribution. In this study, kurtosis of ^{232}Th (− 0.14) and ^{40}K (− 0.33) were found negative which indicate relatively flat distribution while positive kurtosis of ^{226}Ra (0.04) indicate relatively peaked distribution.

Table 4 Statistical data for assessed parameters in sediment samples

Variables	^{226}Ra	^{232}Th	^{40}K
Mean	45.94	50.23	721.27
Median	47.45	49.44	744.07
Std. deviation	9.93	6.76	165.21
Variance	98.63	45.68	27,295.82
Kurtosis	0.04	− 0.14	− 0.33
Skewness	− 0.79	0.33	− 0.51
Minimum	23.54	37.54	354.71
Maximum	59.46	64.37	978.35
Range	35.92	26.83	623.64

Box plot of activity concentration of ^{226}Ra, ^{232}Th, and ^{40}K in becquerels per kilogram is given in Fig. 6. Box plot of activity concentrations gives information about how the values in the data are spread out. As seen in Fig. 6, the median is near the middle of the box for ^{226}Ra and ^{40}K which means the distribution of the data set is normally distributed and symmetric. The median for box plot of ^{232}Th is closer to the bottom of the box, and the distribution is positively skewed. The frequency distribution and Q-Q plots of activity concentrations of ^{226}Ra, ^{232}Th, and ^{40}K were analyzed and are given in Fig. 7, Fig. 8, and Fig. 9, respectively. The graph of ^{232}Th shows that radionuclides demonstrate a normal (bell-shaped) distribution. But ^{226}Ra and ^{40}K show log-normal distribution with some degree of multimodality. The multimodality characteristic shows the complexity of radionuclide in sediment

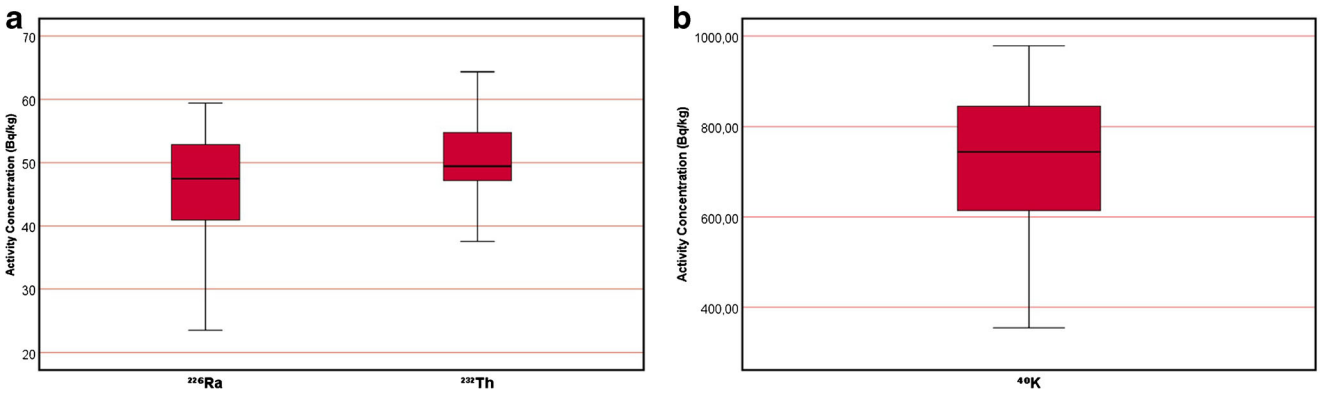

Fig. 6 Box plot of **a** ^{226}Ra and ^{232}Th, **b** ^{40}K

samples. Quantile-quantile plot is another way to identify types of distributions. As can be seen in Figs. 7, 8, and 9, all points lie approximately along 45-degree reference line; it can be assumed that the distributions are normal.

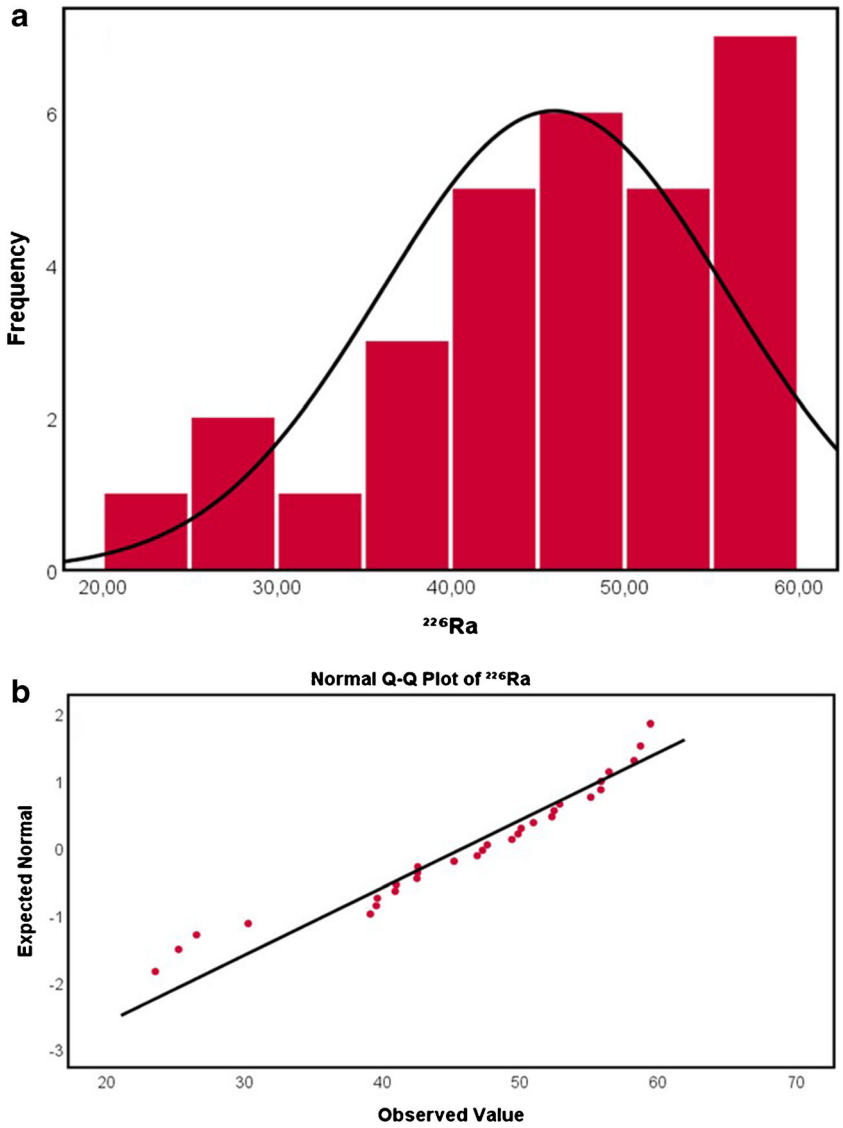

Fig. 7 **a** Frequency distribution and **b** Q-Q plot of ^{226}Ra in sediment samples

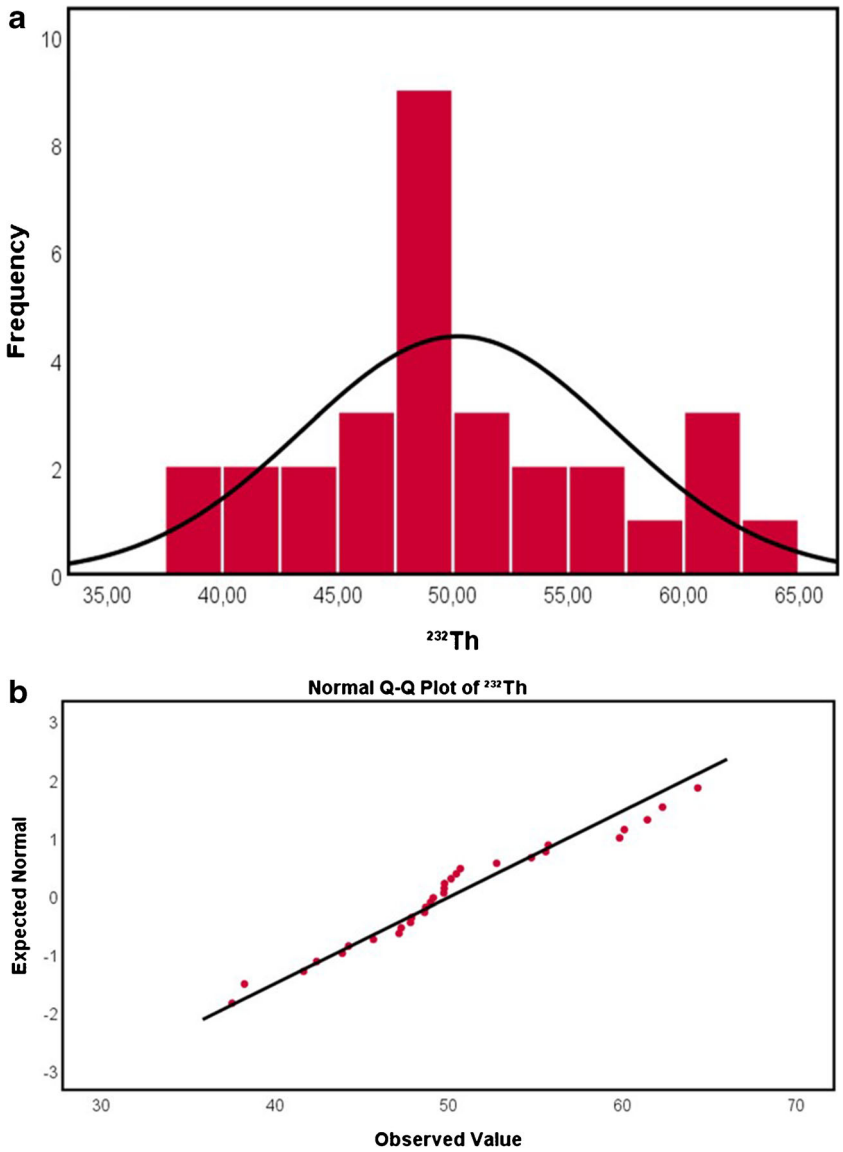

Fig. 8 **a** Frequency distribution and **b** Q-Q plot of ^{232}Th in sediment samples

Linear Pearson's correlation coefficients at alpha testing level of $p < 0.05$ were calculated among radiological parameters for soils around Aliağa Bay and the matrix between radioactive variables is given in Table 5. Strong correlation exists between ^{226}Ra and ^{232}Th ($r = +0.60$), which can be based on their natural origin (Tanasković et al. 2012). Computed correlation between ELCR, D, AEDE, and Ra_{eq} has perfectly positive linearship ($r \geq 0.99$) which means a perfect degree of association between these variables and also strong correlation ($r \geq 0.77$) with ^{226}Ra, ^{232}Th, and ^{40}K.

Factor analysis was also performed on the studied variables by using varimax rotation with Kaiser Normalization method (Sivakumar et al. 2014). The rotated factor 1 and 2 values are listed in Table 6. Factor analysis provided two factors with eigenvalue < 1, explaining 96.74% of the total variance. The rotation space of component 1 and component 2 is given in Fig. 10. As seen in Table 6 and Fig. 10, the first factor accounted for 64.74% of the total variance and mainly characterized by high positive loading of concentrations of ^{232}Th and ^{40}K. The second factor accounted for 31.70% of the total variance and mainly consisted of positive loading of ^{226}Ra. From the overall factor analysis, it can be indicated that ^{232}Th and ^{40}K dominantly increase the radioactivity in the sediments.

In addition, cluster analysis (CA) was performed to understand the similarities between radiological parameters (Fig. 11). The dendrogram shows clusters with similar properties. In the present study, average linkage method was used to measure the distance between clusters. Average linkage method is based on the lowest value of the average distance between clusters in parallel with the single and full link technique. In the dendrogram, all 7 radiological parameters are

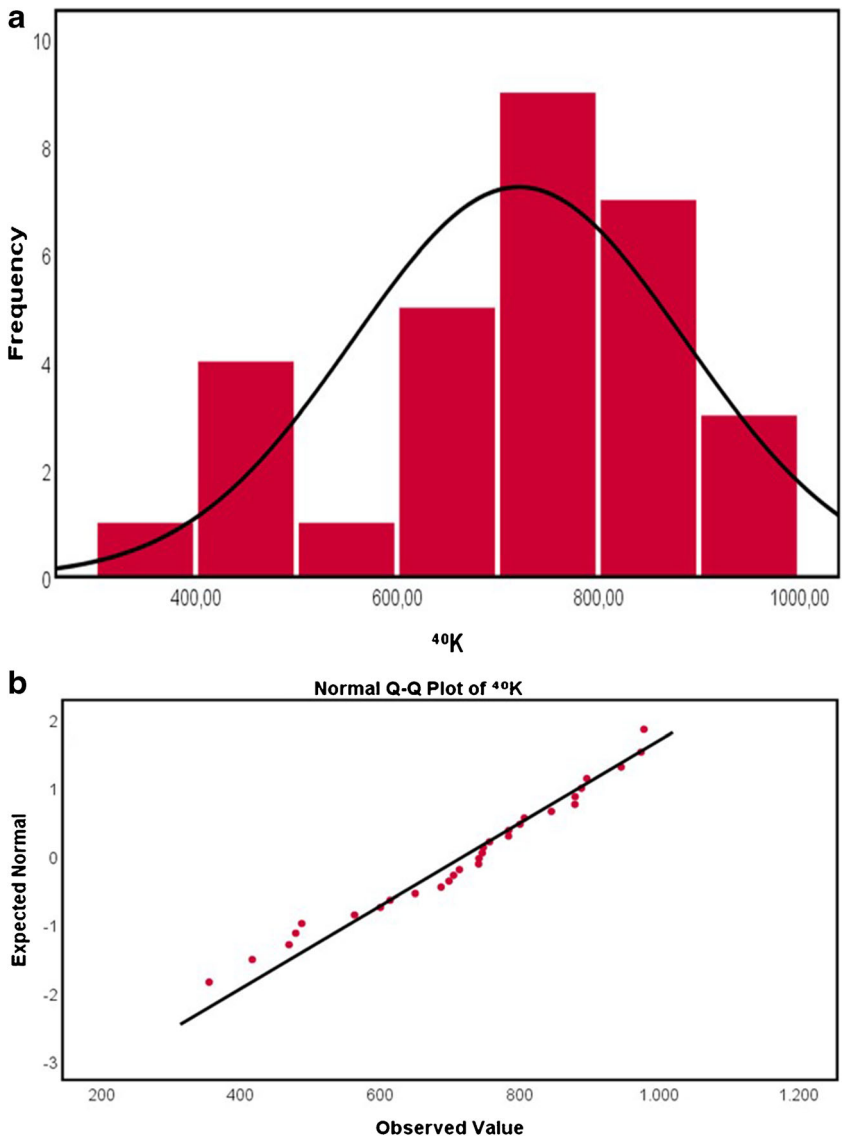

Fig. 9 **a** Frequency distribution and **b** Q-Q plot of ^{40}K in sediment samples

classified into two clusters. Cluster 1 includes high similarity parameters (^{226}Ra and ^{232}Th) which means the radioactivity in sediment samples mainly depends on ^{226}Ra and ^{232}Th activity concentrations (Sivakumar et al. 2014). Cluster II consists of ^{40}K at high Euclidean distance. ELCR, AEDE, D, and Raeq were primarily due to ^{40}K as seen in the dendrogram.

Table 5 Pearson's correlation matrix between radioactive variables of sediment samples around Aliağa Bay

Variables	^{226}Ra	^{232}Th	^{40}K	ELCR	D	AEDE	Ra_{eq}
^{226}Ra	1	0.60	0.70	0.89	0.89	0.89	0.89
^{232}Th	0.60	1	0.50	0.77	0.77	0.77	0.80
^{40}K	0.70	0.50	1	0.91	0.91	0.91	0.89
ELCR	0.89	0.77	0.91	1	1	1	0.99
D	0.89	0.77	0.91	1	1	1	0.99
AEDE	0.89	0.77	0.91	1	1	1	0.99
Ra_{eq}	0.89	0.80	0.89	0.99	0.99	0.99	1

Table 6 Rotated factor loading of the variables

Variables	Component	
	1	2
^{40}K	0.791	0.421
^{226}Ra	0.323	0.940
^{232}Th	0.945	0.180
D	0.853	0.521
AEDE	0.853	0.521
Ra_{eq}	0.828	0.560
H_{ex}	0.828	0.560
ELCR	0.853	0.521
% of variance explained	64.74	31.70

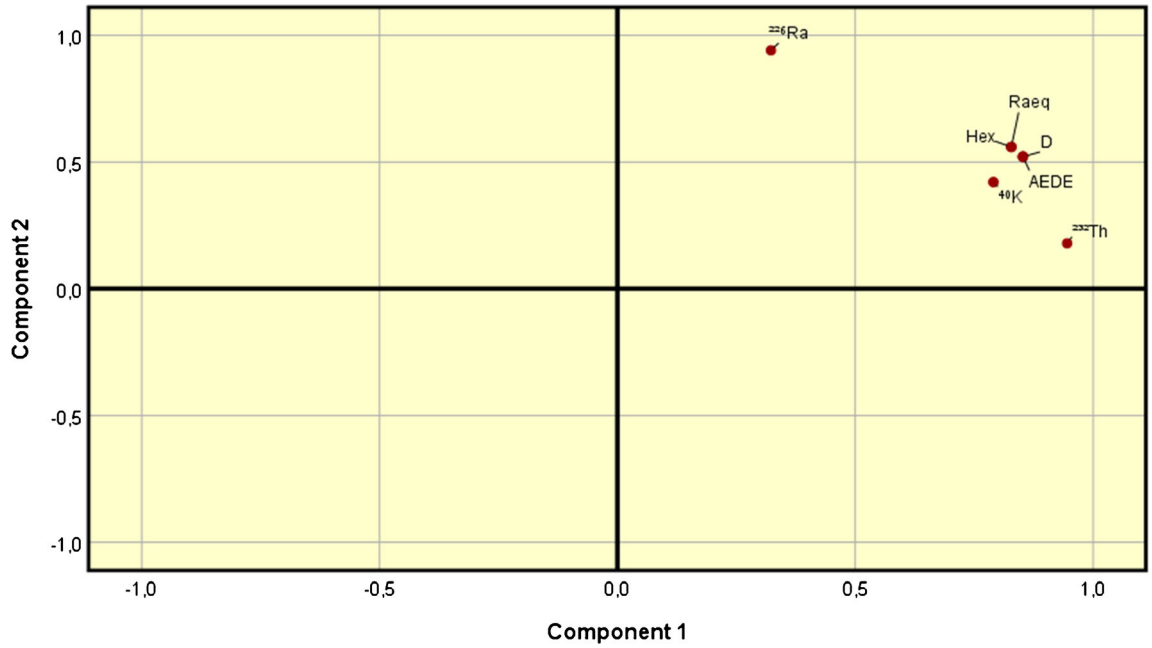

Fig. 10 Graphical representation of components 1 and 2

Conclusions

The activity concentrations have ranges from 23.54 to 59.46 Bq kg^{-1} dry weight for ^{226}Ra, 37.54 to 64.37 Bq kg^{-1} dry weight for ^{232}Th, and 354.71 to 978.35 Bq kg^{-1} dry weight for ^{40}K, respectively. Clearly, the results show that the measured massic activity of ^{40}K significantly exceeds the measured massic activity values of both ^{226}Ra and ^{232}Th. This is an indication that ^{40}K is a more abundant radioactive element than the other elements in the soils under consideration.

The absorbed dose rates due to naturally occurring radionuclides in beaches range between 51.35 and 103.74 nGy h^{-1}. The average absorbed dose rate was found as 81.64 nGy h^{-1} which is higher than the world average absorbed dose rate (UNSCEAR 2000). The annual effective dose ranges from

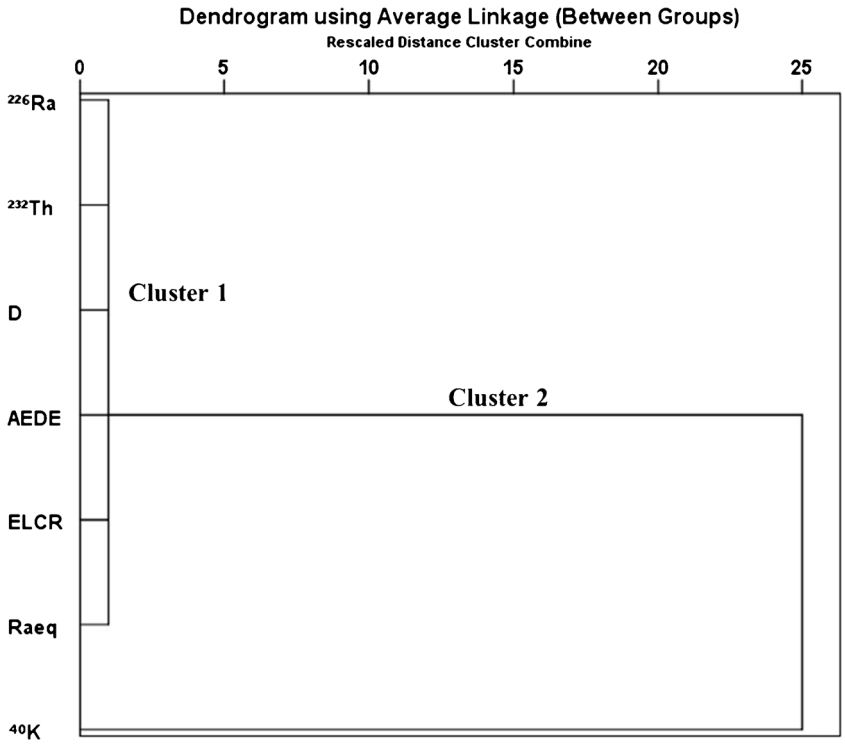

Fig. 11 Dendrogram shows the clustering of radiological parameters

62.98 to 127.23 μSv y^{-1} with a mean value of 100.13 μSv y^{-1}, which is calculated higher than the world average of 70 μSv y^{-1} (UNSCEAR 2000). The radium equivalent activities vary between 110.31 and 219.28 Bq kg^{-1} and average value of radium equivalent activity was calculated to be 173.31 Bq kg^{-1} which is lower than the international recommended maximum value of 370 Bq kg^{-1} (UNSCEAR 2000). The mean excess lifetime cancer risk of sediment samples was found to be 0.40 and changes between 0.25 and 0.51. The mean excess lifetime cancer risk value was found to be higher than the world average of 0.29×10^{-3} according to UNSCEAR (UNSCEAR 2000). From the statistical approach, log-normal distribution of ^{226}Ra and ^{40}K with multimodality shows the complexity characteristic of sediments. The Pearson's correlation coefficient analysis suggested that strong correlation exists between ^{226}Ra and ^{232}Th and in good agreement with CA. CA indicates that ELCR, AEDE, *D*, and Ra_{eq} were primarily due to existence of ^{40}K. From the factor analysis, it can be concluded that ^{232}Th and ^{40}K dominantly increase the radioactivity in the sediment.

This study can be used as a baseline for future researches and the data obtained in this study may be useful for radioactivity mapping. Information obtained from the study was intended to help in the determination of radionuclide sources and radionuclide distribution and potential public health hazard due to radionuclide contamination of the Aliaga Bay, Izmir (Aegean Sea, Turkey).

Acknowledgments The authors are grateful to the Rector of Kirklareli University for his support. Use of facilities at the Central Research Laboratory of Kırklareli University for HPGe detector is acknowledged.

Compliance with ethical standards

Conflict of interest The authors declare that they have no competing interests.

References

Agbalagba EO, Osakwe ROA, Olarinoye IO (2014) Comparative assessment of natural radionuclide content of cement brands used within Nigeria and some countries in the world. J Geochem Explor 142:21–28

Alajeeli A, Elmahroug Y, Mohammed S, Trabelsi A (2019) Determination of natural radioactivity and radiological hazards in soil samples: Alhadba and Abuscabh agriculture projects in Libya. Environ Earth Sci 78(6):194

Albidhani H, Gunoglu K, Akkurt İ (2019) Natural radiation measurement in some soil samples from Basra oil field, IRAQ state. International Journal of Computational and Experimental Science and Engineering (IJCESEN) 5(1):48–51

Al-Hamarneh IF, Awadallah MI (2009) Soil radioactivity levels and radiation hazard assessment in the highlands of northern Jordan. Radiat Meas 44(1):102–110

Al-Obaidi S, Akyıldırım H, Gunoglu K, Akkurt I (2020) Neutron shielding calculation for barite-boron-water. Acta Phys Pol A 137(4):551–553

Al-Trabulsy HA, Khater AEM, Habbani FI (2011) Radioactivity levels and radiological hazard indices at the Saudi coastline of the Gulf of Aqaba. Radiat Phys Chem 80(3):343–348

Altunsoy EE, Tekin HO, Mesbahi A, Akkurt I (2020) MCNPX simulation for radiation dose absorption of anatomical regions and some organs. Acta Phys Pol A 137:561–565

Akkurt İ, Uyanık N, Günoğlu K (2015) Radiation dose estimation: an in vitro measurement for Isparta-Turkey. International Journal of Computational and Experimental Science and Engineering (IJCESEN) 1(1):1–4

Aközcan S (2014) Natural and artificial radioactivity levels and hazards of soils in the Kücük Menderes Basin, Turkey. Environ Earth Sci 71(10):4611–4614

Aközcan S, Külahcı F, Mercan Y (2018) A suggestion to radiological hazards characterization of ^{226}Ra, ^{232}Th, ^{40}K and ^{137}Cs: spatial distribution modelling. J Hazard Mater 353:476–489

Aközcan S, Uğur Görgün A, Yüksel A (2014) Seasonal variation of the concentrations of 137Cs in sediment, sea water, and some organisms collected from Izmir Bay and Didim. Toxicol Environ Chem 96(2): 183–191

Arslan ÖÇ, Boyacioğlu M, Parlak H, Katalay S, Karaaslan MA (2015) Assessment of micronuclei induction in peripheral blood and gill cells of some fish species from Aliağa Bay Turkey. Mar Pollut Bull 94(1-2):48–54

Aydın H, Yürür EE, Uzar S, Küçüksezgin F (2015) Modern dinoflagellate cyst assemblages of Aliağa and Nemrut Bay: influence of industrial pollution. Turk J Fish Aquat Sci 15(3):543–554

Beretka J, Mathew PJ (1985) Natural radioac vity of Australian building materials, industrial wastes and byproducts. Health Phys 48:87–95

Boukhenfouf W, Boucenna A (2011) The radioactivity measurements in soils and fertilizers using gamma spectrometry technique. J Environ Radioact 102(4):336–339

Çam NF, Özken İ, Yaprak G (2013) A survey of natural radiation levels in soils and rocks from Aliağa-Foça region in Izmir, Turkey. Radiat Prot Dosim 155(2):169–180

Currie LA (1968) Limits for qualitative detection and quantitative determination. Application to radiochemistry. Anal Chem 40(3):586–593

Doretti L, Ferrara D, Barison G, Gerbasi R, Battiston G (1992) Natural radionuclides in the muds and waters used in thermal therapy in Abano Terme, Italy. Radiat Prot Dosim 45(1-4):175–178

Ergül HA, Belivermiş M, Kılıç Ö, Topcuoğlu S, Çotuk Y (2013) Natural and artificial radionuclide activity concentrations in surface sediments of Izmit Bay, Turkey. J Environ Radioact 126:125–132

Florou H, Kritidis P (1992) Gamma radiation measurements and dose rate in the coastal areas of a volcanic island, Aegean Sea, Greece. Radiat Prot Dosim 45(1-4):277–279

Ghosh D, Deb A, Bera S, Sengupta R, Patra KK (2008) Measurement of natural radioactivity in chemical fertilizer and agricultural soil: evidence of high alpha activity. Environ Geochem Health 30(1):79–86

Günay O (2018) Assessment of lifetime cancer risk from natural radioactivity levels in Kadikoy and Uskudar District of Istanbul. Arab J Geosci 11(24):782

Günay O, Aközcan S, Kulalı F (2019) Measurement of indoor radon concentration and annual effective dose estimation for a university campus in Istanbul. Arab J Geosci 12(5):171

Günay O, Eke C (2019) Determination of terrestrial radiation level and radiological parameters of soil samples from Sariyer-Istanbul in Turkey. Arab J Geosci 12(20):631

Günay O, Saç MM, İçhedef M, Taşköprü C (2018a) Soil gas radon concentrations along the Ganos Fault (GF). Arab J Geosci 11(9):213

Günay O, Saç MM, Içhedef M, Taşköprü C (2018b) Natural radioactivity analysis of soil samples from Ganos fault (GF). Int J Environ Sci Technol 16:5055–5058. https://doi.org/10.1007/s13762-018-1793-9

Huang Y, Lu X, Ding X, Feng T (2015) Natural radioactivity level in beach sand along the coast of Xiamen Island, China. Mar Pollut Bull 91(1):357–361

Ibraheim NM, Shawky S, Amer HA (1995) Radioactivity levels in Lake Nasser sediments. Appl Radiat Isot 46(5):297–299

ICRP (2007) The 2007 recommendations of the International Commission on Radiological Protection. ICRP publication 103, Ann. ICRP 37:1–332

Khan HM, Chaudhry ZS, Ismail M, Khan K (2010) Assessment of radionuclides, trace metals and radionuclide transfer from soil to food of Jhangar Valley (Pakistan) using gamma-ray spectrometry. Water Air Soil Pollut 213(1-4):353–362

Kolo MT, Amin YM, Khandaker MU, Abdullah WHB (2017) Radionuclide concentrations and excess lifetime cancer risk due to gamma radioactivity in tailing enriched soil around Maiganga coal mine, Northeast Nigeria. International Journal of Radiation Research 15(1):71

Krieger R (1981) Radioactivity of construction materials. Betonw Fert Tech 47(468)

Külahcı F, Aközcan S, Günay O (2020) Monte Carlo simulations and forecasting of radium-226, thorium-232, and potassium-40 radioactivity concentrations. J Radioanal Nucl Chem:1–16

Kulalı F, Günay O, Aközcan S (2019) Determination of indoor radon levels at campuses of Üsküdar and Okan Universities. Int J Environ Sci Technol 16(9):5281–5284

Kurnaz A, Küçükömeroğlu B, Keser R, Okumusoglu NT, Korkmaz F, Karahan G, Çevik U (2007) Determination of radioactivity levels and hazards of soil and sediment samples in Fırtına Valley (Rize, Turkey). Appl Radiat Isot 65(11):1281–1289

Ligero RA, Ramos-Lerate I, Barrera M, Casas-Ruiz M (2001) Relationships between sea-bed radionuclide activities and some sedimentological variables. J Environ Radioact 57(1):7–19

Lu X, Chao S, Ding X (2016) Radiological hazard in the sediment of the Xining section of the Huangshui River, China. Radioprotection 51(1):43–46

Mavi B, Akkurt I (2010) Natural radioactivity and radiation hazards in some building materials used in Isparta, Turkey. Radiat Phys Chem 79(9):933–937

Neşer G, Kontas A, Ünsalan D, Uluturhan E, Altay O, Darılmaz E, Yercan F (2012) Heavy metals contamination levels at the Coast of Aliağa (Turkey) ship recycling zone. Mar Pollut Bull 64(4): 882–887

Nevinsky I, Tsvetkova T, Dogru M, Aksoy E, Inceoz M, Baykara O et al (2018) Results of the simultaneous measurements of radon around the Black Sea for seismological applications. J Environ Radioact 192:48–66

Özseven A, Akkurt I, Günoğlu K (2020) Determination of some dosimetric parameters in Eğirdir Lake, Isparta, Turkey. Int J Environ Sci Technol 17(3):1503–1510

Pazi I, Gonul LT, Kucuksezgin F, Avaz G, Tolun L, Unluoglu A, Olmez G (2017) Potential risk assessment of metals in edible fish species for human consumption from the Eastern Aegean Sea. Mar Pollut Bull 120(1-2):409–413

Qureshi AA, Tariq S, Din KU, Manzoor S, Calligaris C, Waheed A (2014) Evaluation of excessive lifetime cancer risk due to natural radioactivity in the rivers sediments of Northern Pakistan. J Radiat Res Appl Sci 7(4):438–447

Sivakumar S, Chandrasekaran A, Ravisankar R, Ravikumar SM, Prince Prakash Jebakumar J, Vijayagopal P (2014) Measurements of natural radioactivity and evaluation of radiation hazards in coastal sediments of east coast of Tamilnadu, India using statistical approach. Journal of Taibah University for Science 8:375–384

Shouop CJG, Moyo MN, Chene G, Mekontso EJN, Motapon O, Kayo SA, Strivay D (2017) Assessment of natural radioactivity and associated radiation hazards in sand building material used in Douala Littoral Region of Cameroon, using gamma spectrometry. Environ Earth Sci 76(4):164

Sponza D, Karaoğlu N (2002) Environmental geochemistry and pollution studies of Aliağa metal industry district. Environ Int 27(7):541–553

SureshGandhi M, Ravisankar R, Rajalakshmi A, Sivakumar S, Chandrasekaran A, Pream Anand D (2014) Measurements of natural gamma radiation in beach sediments of north east coast of Tamilnadu, India by gamma ray spectrometry with multivariate statistical approach. J Radiat Res Appl Sci 7(1):7–17

Tanasković I, Golobocanin D, Miljević N (2012) Multivariate statistical analysis of hydrochemical and radiological data of Serbian spa waters. J Geochem Explor 112:226–234

Taskin H, Karavus M, Ay P, Topuzoglu A, Hindiroglu S, Karahan G (2009) Radionuclide concentrations in soil and lifetime cancer risk due to gamma radioactivity in Kirklareli, Turkey. J Environ Radioact 100(1):49–53

Tsabaris C, Eleftheriou G, Kapsimalis V, Anagnostou C, Vlastou R, Durmishi C, Kedhi M, Kalfas CA (2007) Radioactivity levels of recent sediments in the Butrint Lagoon and the adjacent coast of Albania. Appl Radiat Isot 65(4):445–453

Tzortzis M, Svoukis E, Tsertos H (2004) A comprehensive study of natural gamma radioactivity levels and associated dose rates from surface soils in Cyprus. Radiat Prot Dosim 109(3):217–224

United Nations. Scientific Committee on the Effects of Atomic Radiation. (2000). Sources and effects of ionizing radiation: sources (Vol. 1). United Nations Publications

Yümün ZÜ, Kam E (2017) Effects of radionuclides on the recent foraminifera from the clastic sediments of the Canakkale Strait-Turkey. J Afr Earth Sci 131:179–182

Zamel AA, Bou-Rabee F, Olszewski M, Bem H (2005) Natural radionuclides and 137 Cs activity concentration in the bottom sediment cores from Kuwait Bay. J Radioanal Nucl Chem 266(2):269–276